nature catalysis

Article

https://doi.org/10.1038/s41929-023-00914-7

Anti-Markovnikov hydrochlorination and hydronitrooxylation of α-olefins via visible-light photocatalysis

Received: 25 May 2022

Accepted: 6 January 2023

Published online: 13 February 2023

Check for updates

Jungwon Kim [1,3], Xiang Sun [1,3], Boris Alexander van der Worp[1,2] & Tobias Ritter [1]

Conventional hydrofunctionalization of α-olefins with mineral acids proceeds with Markovnikov selectivity to afford branched isomers. The direct formation of linear constitutional isomers is challenging, yet anti-Markovnikov addition would be valuable for the synthesis of commodity chemicals, such as primary alcohols, which are currently only accessible via stoichiometric redox reactions, with a full equivalent of waste of both oxidant and reductant. Strategies that utilize radical intermediates have been demonstrated, but only for activated alkenes, and the direct use of aqueous mineral acids remains elusive. Here we present anti-Markovnikov addition reactions of aqueous hydrochloric and nitric acid to unactivated alkenes. The transformation is enabled by the in situ generation of photoredox-active ion pairs, derived from acridine and the mineral acid, as a combined charge- and phase-transfer catalyst. The introduction of a hydrogen atom transfer catalyst enabled us to bypass the challenging chain propagation by hydrochloric and nitric acids that originates from the high bond dissociation energy.

Alpha (α)-olefins are unactivated alkenes of the formula C_nH_{2n}. Their hydrofunctionalization is one of the fundamental reaction classes already taught in introductory chemistry courses, when the concept of Markovnikov selectivity in alkene hydrochlorination to afford branched isomers is introduced[1]. Access to the linear anti-Markovnikov products cannot proceed selectively through an analogous mechanism due to the high energy of the primary carbocations. Access to anti-Markovnikov products is commonly accomplished by two-step redox processes (Fig. 1a). For example, alkene hydroboration followed by oxidation is a robust two-step sequence to achieve hydration[2] or hydrochlorination[3]. Although the two-step sequence is efficient and acceptable for fine chemical synthesis, in which expensive, functionalized molecules are further derivatized, multiple-step syntheses or the use of expensive reagents are cost prohibitive for the synthesis of commodity chemicals, such as addition reactions to α-olefins. For example, primary alcohols are produced on a million-tonne scale annually[4] by the Ziegler process through stoichiometric hydroalumination followed by oxidation by molecular oxygen, with stoichiometric aluminium oxide as a by-product[5]. Likewise, all the reported catalytic approaches to anti-Markovnikov hydrochlorination and hydrooxygenation of α-olefins share the same requirement for both stoichiometric oxidation and stoichiometric reduction, which is not desirable for a sustainable, overall redox-neutral process (Fig. 1a)[6–10]. Impressive direct and catalytic anti-Markovnikov addition reactions of a number of nucleophiles, which include amines[11–13], thiols[14] and silanes[15], to unactivated olefins were reported[16,17], but the corresponding reactions to make C–Cl or C–O bonds remain elusive. Hydrochlorination and hydrooxygenation of styrenes (Fig. 1b)[18,19] were established with modern photoredox chemistry that enables the remarkable single-electron oxidation of the styrene substrate; however, anti-Markovnikov hydrochlorination and hydrooxygenation of α-olefins are currently beyond the scope of known reaction chemistry, in part because the single-electron oxidation of

[1]Max-Planck-Institut für Kohlenforschung, Mülheim, Germany. [2]Institute of Organic Chemistry, RWTH Aachen University, Aachen, Germany. [3]These authors contributed equally: Jungwon Kim and Xiang Sun. e-mail: ritter@kofo.mpg.de

https://doi.org/10.1038/s41929-023-00914-7

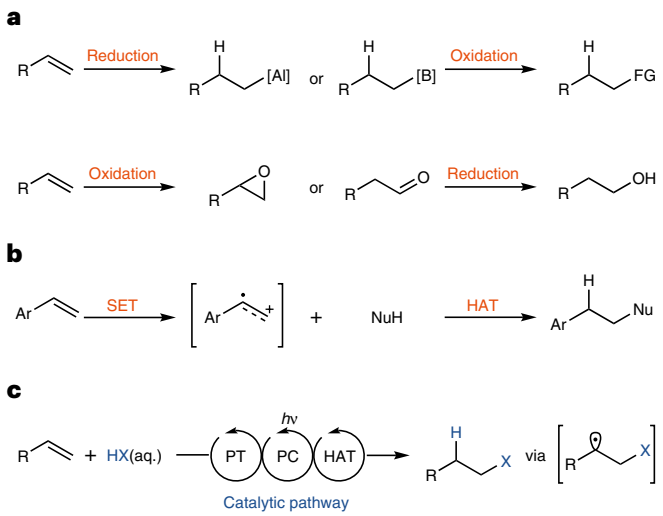

Fig. 1 | Anti-Markovnikov hydrofunctionalization of alkenes. a, Syntheses of anti-Markovnikov compounds from alkenes via two-step redox processes (FG = Cl or OH). **b**, Catalytic anti-Markovnikov hydrofunctionalizations of styrenes. **c**, A proposed pathway for the ideal radical anti-Markovnikov hydrofunctionalization with HX (X = Cl or ONO_2). PC, photoredox catalysis; PT, phase transfer.

α-olefins is thermodynamically more challenging by about 0.8 V than the oxidation of styrene[20]. Success in this area is relevant because it would illustrate an approach to the hydration of unactivated olefins without stoichiometric waste. A promising strategy to directly access anti-Markovnikov addition products entails the generation of radicals ($X^{\cdot}$), which has been successfully developed for hydrobromination[21]. Such chemistry is not yet available for hydrochlorination and hydrooxygenation reactions presumably due to the redox properties and H–X bond strengths of the involved reagents. For example, the H–Br bond dissociation energy (BDE) of 88 kcal mol^{-1} (ref. [22]) is sufficiently small to engage in hydrogen atom transfer (HAT) to carbon-centred radicals, initially formed on bromine radical addition to olefins[21]. Hydrochloric acid has a higher BDE (103 kcal mol^{-1}) (ref. [22]), as do many oxygen-based reagents, such as HNO_3 (BDE = 102 kcal mol^{-1}) (ref. [22]), and, therefore, cannot engage in such HAT reactions[23]. In addition, access to the radicals $X^{\cdot}$ by single-electron oxidation is more facile for compounds with lower reduction potentials, for example, the bromide anion is more readily oxidized than oxygen-based compounds, such as nitrate or water ($E°$ ($Br^{\cdot}/Br^{-}$) = 1.9 V versus NHE (normal hydrogen electrode) in water; $E°$ ($NO_3^{\cdot}/NO_3^{-}$) = 2.5 V versus NHE in water; $E°$ ($OH^{\cdot}/H_2O$) = 2.7 V versus NHE in water)[24]. Here we realized the anti-Markovnikov hydrofunctionalization reactions of unactivated olefins with technical, aqueous hydrochloric and nitric acids through phase transfer and visible-light photoredox catalysis[25] without the need for any other stoichiometric reagent, except solvent (Fig. 1c).

Results

Design of the system

We attempted to identify a photoredox catalyst that could also function as a phase-transfer catalyst as shown in Fig. 2a for the transfer of polar HX from an aqueous solution to an apolar liquid phase that contained the α-olefin. Subsequent generation of $X^{\cdot}$ from the anion X^{-} by single-electron transfer (SET) would circumvent the challenging homolytic cleavage of HX. A suitable base B that would lead to a photoredox-active catalyst BH^{+} on protonation by HX could form a lipophilic ion pair $BH^{+}X^{-}$ with an accessible anion X^{-} for oxidation by SET. Nitrogen-arylated 9-arylacridiniums are common photoredox catalysts[20,25] but cannot function as suitable base and would require an efficient anion exchange to generate an ion pair with an anion X^{-} for oxidation by SET. Therefore, we selected a 9-arylacridine (**1**), which itself does not function as a photoredox catalyst but can be protonated by HX to lead to a photoredox-active acridinium catalyst with an X^{-} counteranion ($\mathbf{I}^{+}X^{-}$) for phase transfer (Fig. 2a). SET within the ion pair of excited $\mathbf{I}^{+}X^{-}$ could occur to form electrophilic radicals such as $NO_3^{\cdot}$ and $Cl^{\cdot}$. The generated radical $X^{\cdot}$ might subsequently add to the terminal position of alkene[26], followed by polarity-matched HAT from a thiol catalyst (the BDE of CH_3S–H = 87 kcal mol^{-1}) (ref. [22]) to the carbon-centred radical **III**, which leads to the product. Regeneration of both catalysts could be achieved via SET from the acridine radical **II** to the thiyl radical and subsequent protonation of thiolate by HX[20]. The protonation of precatalyst **1** would therefore not only generate X^{-} from HX, which, as opposed to HX, is oxidizable, but also ensure the proximity between the acridinium cation $\mathbf{I}^{+}$ and X^{-}, which is not the case with conventional cationic photoredox catalysts and constitutes the conceptual advance disclosed here. HAT from both the weak allylic C–H bond of the alkene and the thiol to the radical $X^{\cdot}$ must be slower than radical addition, the deleterious addition of thiyl radicals to alkenes by the thiol-ene reaction must be slower[14] and the potential rate-limiting HAT from thiol to the carbon-centred radical **III** may render the higher thermodynamic stability of the anti-Markovnikov-based intermediate **III** irrelevant if under Curtin–Hammett control (vide infra). Our approach differs conceptually from prior art in that the phase transfer from an aqueous mineral acid enables a direct mineral anion oxidation within a photoactive ion pair, as opposed to oxidation of the substrate by a photoredox catalyst, for example, as in the case of styrene hydrochlorination (Fig. 1b)[18]. Previously, 9-arylacridine (**1**) was used as a photoredox catalysts in conjunction with carboxylic acids to produce alkyl radicals through a proton-coupled electron transfer mechanism[27,28], which differs conceptually from our work in the sense that the key photoredox-active ion pair with a protonated acridine as shown here is not formed; the proton-coupled electron transfer approach with carboxylic acid does not afford anti-Markovnikov addition to olefins (Supplementary Tables 14 and 15).

Reaction development

Experimental execution of the rationale resulted in the selective anti-Markovnikov hydrochlorination and hydronitrooxylation of terminal olefins catalysed by a combination of 9-(2-chlorophenyl)acridine (**1**) as the pre-photoredox catalyst, and thiol or disulfide as the HAT catalyst under visible light irradiation (Fig. 2b). In line with our hypothesis, the use of the basic acridine catalyst **1** is crucial to observe the desired reactivity, whereas conventional N-substituted acridinium-based photoredox catalysts, such as 9-mesityl-10-methylacridinium tetrafluoroborate (Fukuzumi's catalyst) or 9-mesityl-2,7-dimethyl-10-phenylacridinium tetrafluoroborate (Nicewicz's catalyst) did not afford products with aqueous mineral acids or 4-chloropyridine hydrochloride (Supplementary Table 6). Yet, comparable productive reactivity was observed when a photocatalyst with a chloride counteranion, such as $[Ir(dFCF_3ppy)_2(dtbbpy)]Cl$ ($dFCF_3ppy$, 3,5-difluoro-2-(5-(trifluoromethyl)-2-pyridinyl); dtbbpy, di-*tert*-butyl-2,20-bipyridine), was used together with 4-chloropyridine hydrochloride as the HCl surrogate (Supplementary Table 6). The formation of ion pairs for phase transfer with the photoredox-active cation and the mineral-acid-derived anion X^{-} appears important given that the efficiency of the reaction decreases on the addition of redox-inactive anion sources, such as tetra-*n*-butylammonium (TBA) tetrafluoroborate (Supplementary Table 7). These results clearly demonstrate the conceptual advance in the use of acridine catalyst **1** to afford ion pair $\mathbf{I}^{+}X^{-}$ directly from HX, whereas conventional acridinium-based photoredox catalysts cannot provide the corresponding ion pairs efficiently. Acridinium-based photoredox catalysts were previously shown to generate chlorine and nitrate radicals[29–31], but in the absence of ion pairs that reactivity is not sufficient for hydrofunctionalization of unactivated alkenes. Control experiments confirmed that acridine,

https://doi.org/10.1038/s41929-023-00914-7

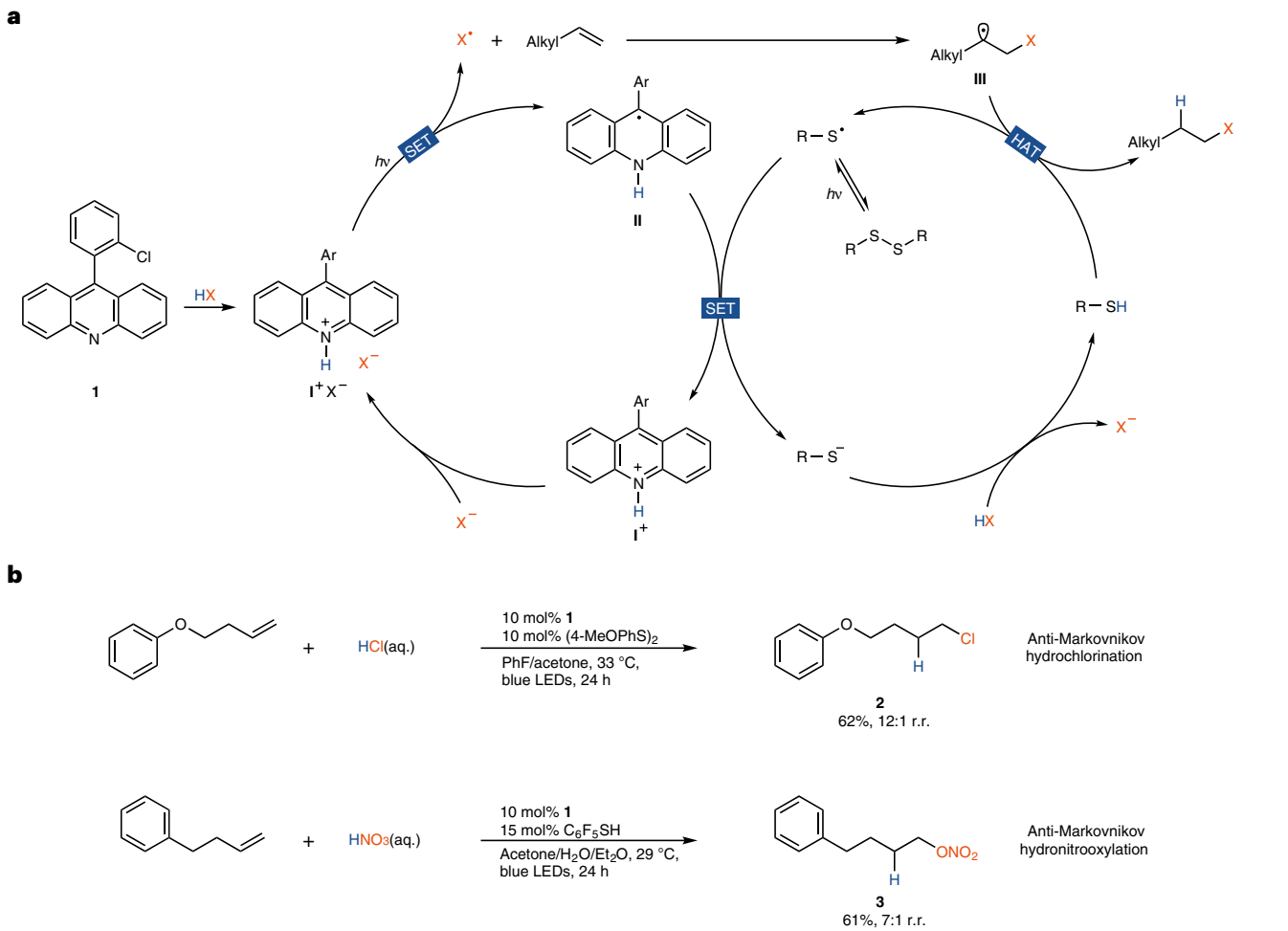

Fig. 2 | Anti-Markovnikov addition of HX to unactivated olefins. a, Proposed catalytic cycle. **b**, Transformations of homoallyl phenyl ether to give the primary alkyl chloride **2** (top) and 4-phenyl-1-butene to give the primary alkyl nitrate **3** (bottom). r.r., regioselectivity ratio.

thiol and light are all essential for anti-Markovnikov addition, and no considerable background reaction was observed otherwise under the reaction conditions with the selected solvents (Supplementary Tables 1, 6, 8 and 13). Under the reaction conditions, nitrate proved uniquely productive when compared to other oxygen-based anions, such as acetate or trifluoroacetate, possibly a consequence of different reaction kinetics with respect to those of olefin addition and hydrogen atom abstraction.

Substrate scope evaluation

As depicted in Figs. 3 and 4a, simple α-olefins were hydrochlorinated and hydronitrooxylated (**4** and **27**) with a preference of roughly one order of magnitude for the linear isomer. When the reaction was executed on a 10 mmol scale, the anti-Markovnikov product, for example, **27**, could be purified to give a single isomer by distillation. For acid-sensitive substrates, HCl can be substituted with pyridinium hydrochloride (for example, **12**). Yet, several functional groups, such as ester, sulfonate, sulfonamide, silyl, ketone, nitrile and carboxylic acid, were even compatible with aqueous mineral acid, possibly a consequence of the biphasic reaction system with an appropriate phase transfer. Heteroarene-bearing olefins could also be utilized in the reactions, and no signs of the radical addition to aromatic rings were observed (**15**–**17** and **25**). Internal olefins participated in the reaction but provided, as expected, a near equal mixture of constitutional isomers (**22** and **39**). Even 1,1-disubstituted olefins were hydrofunctionalized regioselectively, which is striking given the potential formation of tertiary carbocations through olefin protonation by the strong acid (**20**, **21**, **23**, **35**–**38**, **40** and **41**). Cyclic 1,1-disubstituted and trisubstituted alkenes reacted with Markovnikov selectivity or were isomerized, which may be explained by the higher stability of the intermediate cation on protonation (Supplementary Fig. 3). Regioselective hydrofunctionalization of allylbenzene was beyond the scope of the reaction (**18**), possibly due to a competing HAT from the weak benzylic as well as allylic C–H bond (BDE = 82 kcal mol^{-1}) (ref. [32]). Alkyl chlorides can be further functionalized in nucleophilic substitution reactions[10] or used as alkyl radical precursors[33,34]. In addition, conversion of the nitrate esters into alcohol, iodide and thiocyanate was accomplished, as shown in Fig. 4b.

Mechanistic investigations

Preliminary mechanistic studies (Fig. 5) are in agreement with the proposed cycle shown in Fig. 2. The addition of HCl or 4-chloropyridine hydrochloride to a solution of **1** resulted in an increase in absorption between 390 and 460 nm as compared with that of **1** (Supplementary Fig. 5). Stern–Volmer quenching experiments cannot, by definition, be conducted with the ion pairs relevant to the reaction, but even the results with the in situ generated $\mathbf{I}^+BF_4^-$ and quenchers (Cl^-, NO_3^- and 1-dodecene) are consistent with the reductive quenching of $\mathbf{I}^+$ by either Cl^- or NO_3^- (Fig. 5a). Radical trapping experiments with 1,1-dichloro-2-vinylcyclopropane further substantiated the formation of $Cl^{\cdot}$ and $NO_3^{\cdot}$ from the reductive quenching process (Fig. 5b).

https://doi.org/10.1038/s41929-023-00914-7

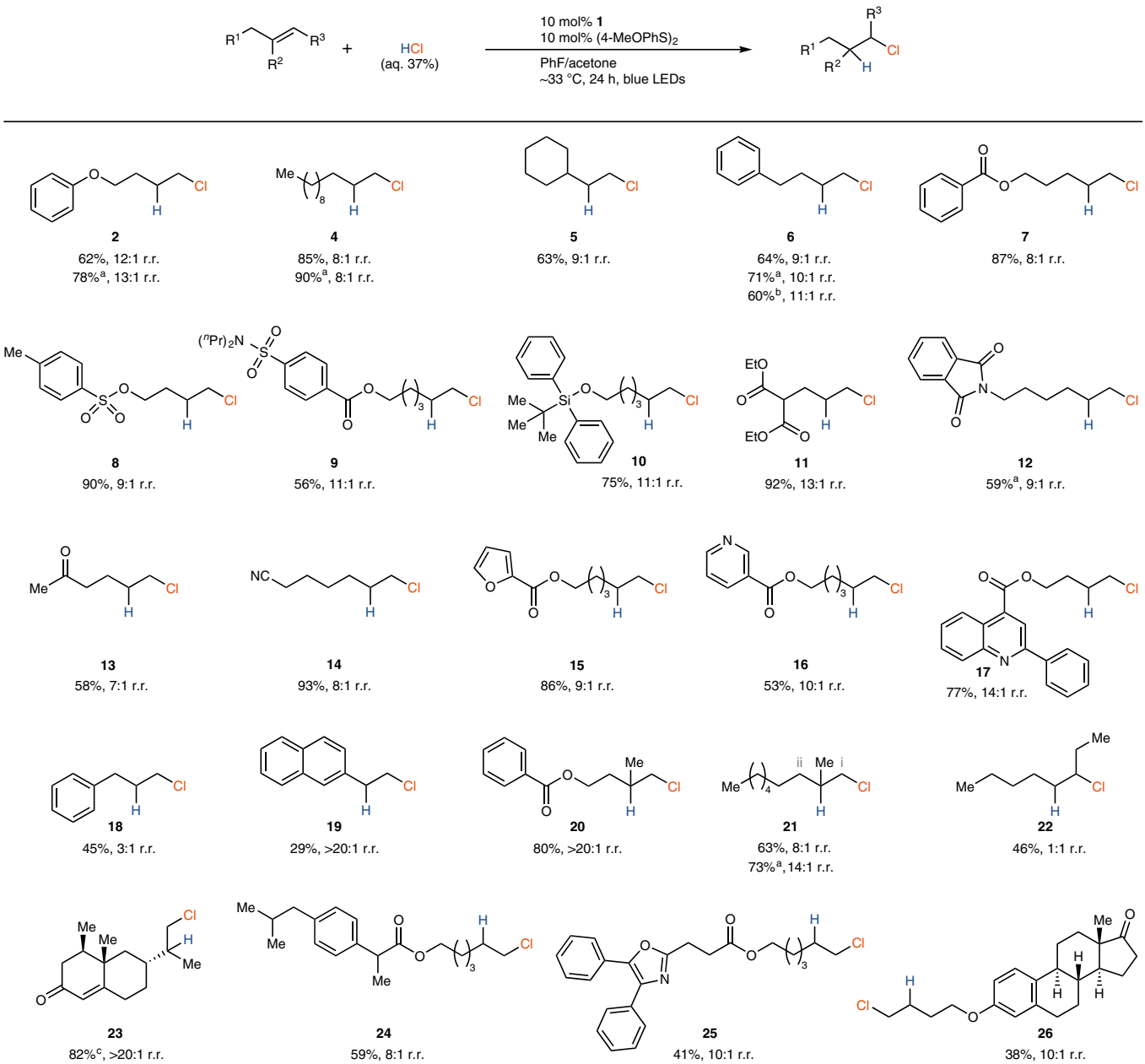

Fig. 3 | Reactivity evaluation of anti-Markovnikov hydrochlorination. Reaction conditions: alkene (0.3 mmol), HCl(aq. 37%) (0.45 mmol), **1** (10 mol%), bis(4-methoxyphenyl) disulfide (10 mol%) in fluorobenzene/acetone (3 ml, 5:1 v/v) at 33 °C under 2 × 40 W blue light-emitting diodes (LEDs) for 24 h. i and ii denote the site of Cl of the major/minor products. See Supplementary Methods for the detailed experimental procedure. [a]Reaction performed with 4-chloropyridine hydrochloride (0.45 mmol). [b]Reaction performed on a 1.2 mmol scale, 48 h. [c]Diastereomeric ratio = 1:1.

Density functional theory (DFT) analysis is consistent with a near barrierless addition of $Cl^{\cdot}$ to olefin, specifically 1-butene in the calculation. A smooth, monotonous potential energy surface was observed for the addition, and all the attempts to locate a transition state failed (Supplementary Fig. 15), while HAT to the crotyl radical was affiliated with a small but notable barrier (Fig. 5c). Although we initially attempted to target anti-Markovnikov selectivity through the stability difference between the more stable internal carbon radical and the terminal radical, for example, Int_{linear}, versus $Int_{branched}$ (Fig. 5e), DFT analysis indicates that the selectivity is explained by the Curtin–Hammett principle. Interconversion of the two carbon radicals via a 1,2-chlorine shift[35] is fast with a computed barrier of $\Delta G^{\ddagger} = 8.2$ kcal mol^{-1} compared to that of the irreversible HAT from thiol to product. The difference in energy of the two computed transition states to afford linear and branched products (P_{linear} and $P_{branched}$, respectively) is $\Delta G_{TS_{branched}} - \Delta G_{TS_{linear}} = 1.5$ kcal mol^{-1}, in agreement with the experimentally observed selectivity (Fig. 5e).

The reaction between $NO_3^{\cdot}$ and 1-butene also shows a near-barrierless addition process (Supplementary Fig. 16), in contrast to that of HAT to the crotyl radical (Fig. 5d). Although similar to the energy surface for hydrochlorination, interconversion of the two $NO_3^{\cdot}$/1-butene adducts $Int_{linear,nit}$ and $Int_{branched,nit}$ (Fig. 5f) shows a higher energy barrier than that to the products by HAT. Therefore, the regioselectivity in the hydronitrooxylation reaction seems to be governed by the rates of nitrate radical addition to the olefin. Although the difference of the energies of the terminal and internal carbon radical $\Delta G_{Int_{branched,nit}} - \Delta G_{Int_{linear,nit}} = 0.7$ kcal mol^{-1} is in agreement with the experimentally observed selectivity of ~7:1, a statistical analysis of

https://doi.org/10.1038/s41929-023-00914-7

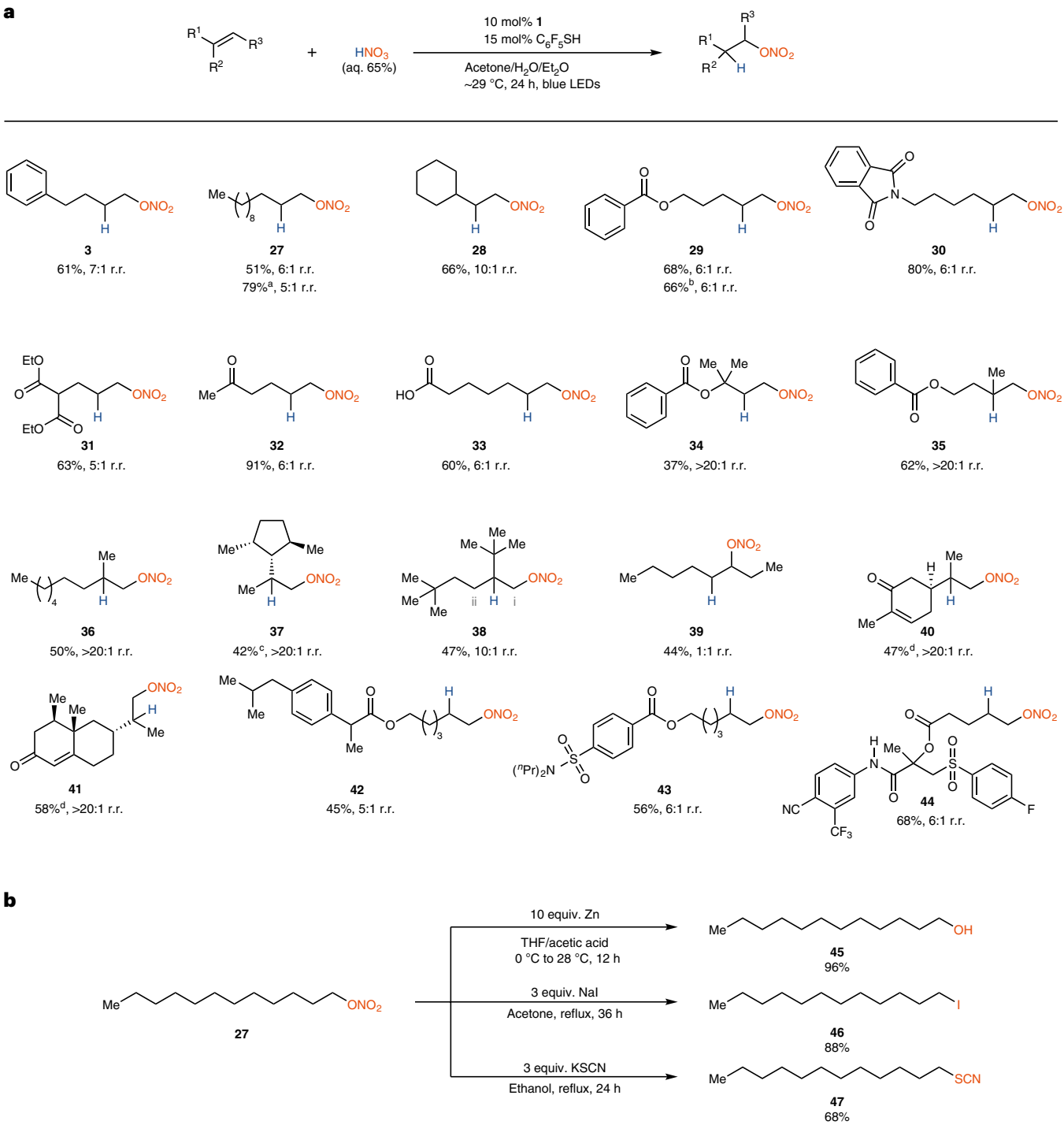

Fig. 4 | Reactivity evaluation of anti-Markovnikov hydronitrooxylation. **a**, Hydronitrooxylation with HNO_3. Reaction conditions: alkene (0.2 mmol), HNO_3(aq. 65%) (0.60 mmol), **1** (10 mol%), pentafluorothiophenol (15 mol%) in acetone/H_2O/diethyl ether (2.6 ml, 10:2:1 v/v/v) at 29 °C under 40 W blue LEDs for 24 h. i and ii denote the site of ONO_2 of the major/minor products. See Supplementary Methods for the detailed experimental procedure. **b**, Further transformations with alkyl nitrate **27**. [a]Reaction performed on a 10 mmol scale, 48 h. [b]Reaction performed on a 1.0 mmol scale. [c]Diastereomeric ratio = 2:1. [d]Diastereomeric ratio = 1:1.

reaction kinetics by transition-state theory was not performed due to the absence of computationally accessible transition states for the barrierless addition process.

Conclusions

Direct hydrochlorination of α-olefins with aqueous HCl is achieved via visible-light photoredox catalysis. The demonstrated concept was extended to hydrooxygenation and may be helpful to approach the long-lasting challenge of the anti-Markovnikov hydration of α-olefins.

Methods

General procedure for anti-Markovnikov hydrochlorination

Under an ambient atmosphere, to an oven-dried 4 ml borosilicate vial equipped with a magnetic stir bar were added alkene (0.300 mmol,

https://doi.org/10.1038/s41929-023-00914-7

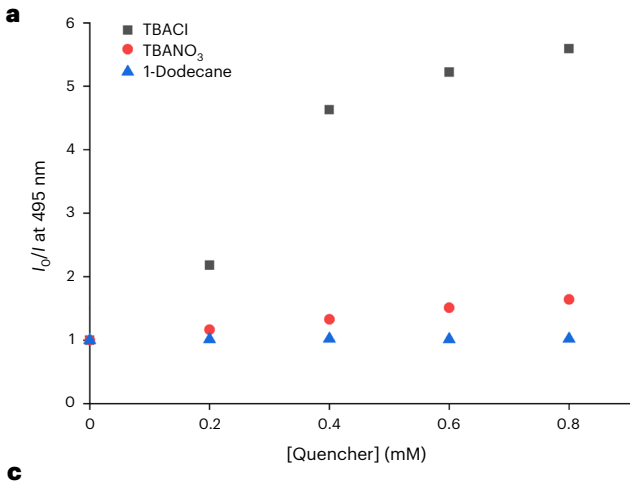

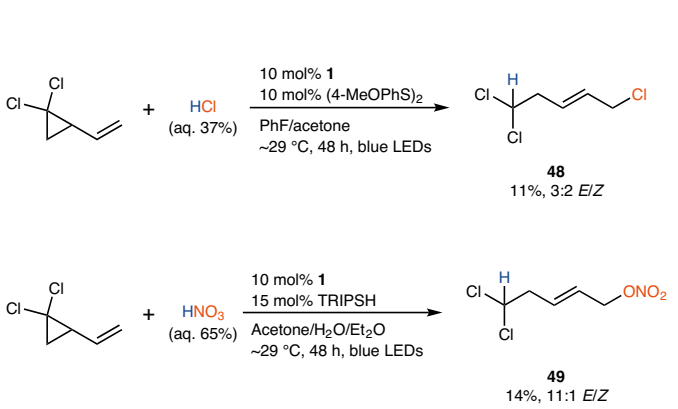

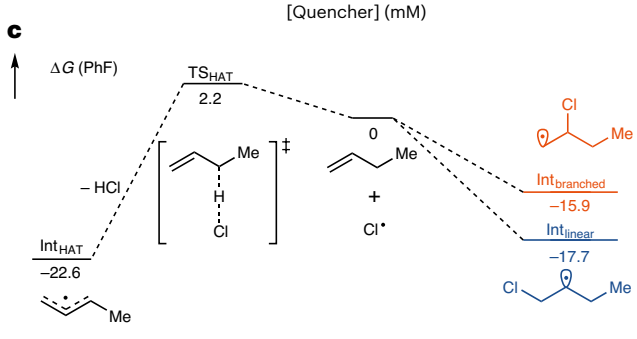

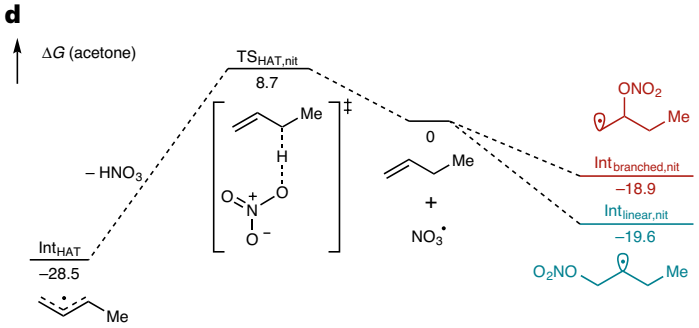

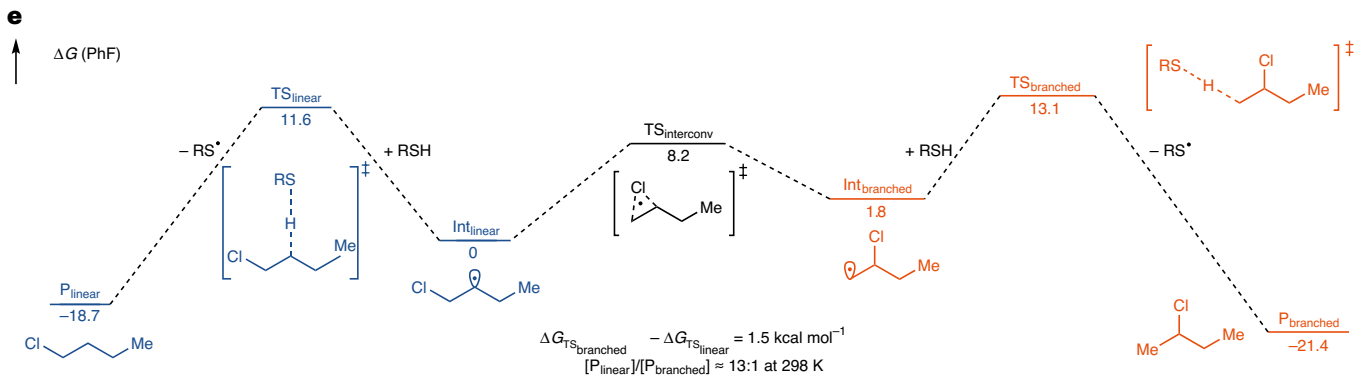

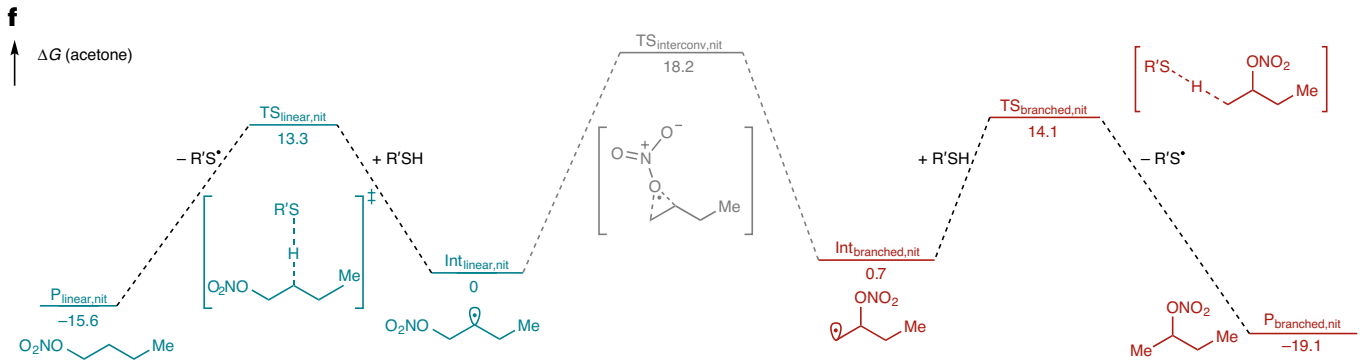

Fig. 5 | Mechanistic investigations. a, Stern–Volmer plot of in situ generated $I^+BF_4^-$ luminescence quenching by TBACl, $TBANO_3$ and 1-dodecene. I_0, luminescence intensity without quencher; I, luminescence intensity with quencher. **b**, Radical trapping experiments with 1,1-dichloro-2-vinylcyclopropane. Reaction conditions for hydrochlorination: alkene (1.0 mmol), HCl(aq. 37%) (1.5 mmol), **1** (10 mol%), bis(4-methoxyphenyl) disulfide (10 mol%) in fluorobenzene/acetone (10 ml, 5:1 v/v) at 29 °C under 40 W blue LED for 48 h. Reaction conditions for hydronitrooxylation: alkene (1.0 mmol), HNO_3(aq. 65%) (3.0 mmol), **1** (10 mol%), 2,4,6-triisopropylthiophenol (TRIPSH, 15 mol%) in acetone/H_2O/diethyl ether (13 ml, 10:2:1 v/v/v) at 29 °C under 40 W blue LED for 48 h. See Supplementary Methods for the detailed experimental procedure. **c**, DFT-calculated energy profiles (kcal mol^{-1}) for the reaction of $Cl^•$ with 1-butene. **d**, DFT-calculated energy profiles (kcal mol^{-1}) for the reaction of $NO_3^•$ with 1-butene. **e**, DFT-calculated energy profiles (kcal mol^{-1}) for the reaction of carbon-centred radical intermediates (Int_{linear} and $Int_{branched}$) and 4-methoxythiophenol (RSH). **f**, DFT-calculated energy profiles (kcal mol^{-1}) for the reaction of carbon-centred radical intermediates ($Int_{linear,nit}$ and $Int_{branched,nit}$) and pentafluorothiophenol (R'SH).

1.00 equiv.), **1** (8.7 mg, 30 µmol, 10 mol%), bis(4-methoxyphenyl) disulfide (8.4 mg, 30 µmol, 10 mol%) and fluorobenzene/acetone (3.0 ml, 5:1 v/v, 0.10 M). Aqueous HCl (37%, 37 µl, 44 mg, 0.45 mmol, 1.5 equiv.) was added to the reaction mixture via a micropipette, whereupon the colour of the solution turned yellow. The vial was sealed with a septum cap, and a gentle stream of argon was passed through the solution via a needle (*Φ* 0.80 × 120 mm) for 1 min. Thereafter, the vial was placed in the middle of two blue LEDs (2.5 cm away from each LED) and irradiated for 24 h. The temperature of the reaction mixture was kept at approximately 33 °C through cooling with a fan. Then, the reaction mixture was concentrated under reduced pressure, and the residue was purified by flash column chromatography on silica gel to afford the desired product. If necessary, $AgNO_3$-impregnated silica gel (~10%) was utilized for the purification process.

General procedure for anti-Markovnikov hydronitrooxylation

Under an ambient atmosphere, to an oven-dried 4 ml borosilicate vial equipped with a magnetic stir bar were added alkene (0.200 mmol, 1.00 equiv.), **1** (5.8 mg, 20 µmol, 10 mol%), pentafluorothiophenol (4.0 µl, 6.0 mg, 30 µmol, 15 mol%) and acetone/water/diethyl ether (2.6 ml, 10:2:1 v/v/v, 77 mM). Aqueous HNO_3 (65%, 41 µl, 58 mg, 0.60 mmol, 3.0 equiv.) was added to the reaction mixture via micropipette, whereupon the colour of the solution turned yellow. The vial was sealed with a septum cap, and a gentle stream of argon was passed through the solution via a needle (*Φ* 0.80 × 120 mm) for 1 min. Thereafter, the vial was placed 2.5 cm away from a blue LED and irradiated for 24 h. The temperature of the reaction mixture was kept at approximately 29 °C through cooling with an air flow. Then, the reaction mixture was diluted with diethyl ether (3 ml) and washed with saturated aqueous Na_2CO_3 solution (3 ml). The aqueous phase was further extracted with diethyl ether (3 ml). The combined organic phase was dried over $MgSO_4$ and filtered. Then, the solvent was removed under reduced pressure. The residue was purified by flash column chromatography on silica gel to afford the desired product. If necessary, $AgNO_3$-impregnated silica gel (~10%) was utilized for the purification process.

Data availability

All data relating to the materials and methods, optimization studies, experimental procedures, DFT calculations and NMR spectra are available in the Supplementary Information or from the authors upon reasonable request.

References

1. Markownikoff, W. I. Ueber die Abhängigkeit der verschiedenen Vertretbarkeit des Radicalwasserstoffs in den isomeren Buttersäuren. *Justus Liebigs Ann. Chem.* **153**, 228–259 (1870).
2. Brown, H. C. & Rao, B. C. S. A new technique for the conversion of olefins into organoboranes and related alcohols. *J. Am. Chem. Soc.* **78**, 5694–5695 (1956).
3. Brown, H. C. & De Lue, N. R. Organoboranes for synthesis. 12. The reaction of organoboranes with nitrogen trichloride. A convenient procedure for the conversion of alkenes into alkyl chlorides via hydroboration. *Tetrahedron* **44**, 2785–2792 (1988).
4. Noweck, K. & Grafahrend, W. in *Ullmann's Encyclopedia of Industrial Chemistry* Vol. 14, 117–141 (Wiley, 2012).
5. Ziegler, K., Krupp, F. & Zosel, K. Eine einfache Synthese primärer Alkohole aus Olefinen. *Angew. Chem.* **67**, 425–426 (1955).
6. Dong, G., Teo, P., Wickens, Z. K. & Grubbs, R. H. Primary alcohols from terminal olefins: formal anti-Markovnikov hydration via triple relay catalysis. *Science* **333**, 1609–1612 (2011).
7. Liu, W., Li, W., Spannenberg, A., Junge, K. & Beller, M. Iron-catalysed regioselective hydrogenation of terminal epoxides to alcohols under mild conditions. *Nat. Cat.* **2**, 523–528 (2019).
8. Yao, C., Dahmen, T., Gansäuer, A. & Norton, J. Anti-Markovnikov alcohols via epoxide hydrogenation through cooperative catalysis. *Science* **364**, 764–767 (2019).
9. Lai, S.-Q., Wei, B.-Y., Wang, J.-W., Yu, W. & Han, B. Photocatalytic anti-Markovnikov radical hydro- and aminooxygenation of unactivated alkenes tuned by ketoxime carbonates. *Angew. Chem. Int. Ed.* **60**, 21997–22003 (2021).
10. Li, X., Jin, J., Chen, P. & Liu, G. Catalytic remote hydrohalogenation of internal alkenes. *Nat. Chem.* **14**, 425–432 (2022).
11. Utsunomiya, M. & Hartwig, J. F. Ruthenium-catalyzed anti-Markovnikov hydroamination of vinylarenes. *J. Am. Chem. Soc.* **126**, 2702–2703 (2004).
12. Musacchio, A. J. et al. Catalytic intermolecular hydroaminations of unactivated olefins with secondary alkyl amines. *Science* **355**, 727–730 (2017).
13. Park, S., Jeong, J., Fujita, K.-I., Yamamoto, A. & Yoshida, H. Anti-Markovnikov hydroamination of alkenes with aqueous ammonia by metal-loaded titanium oxide photocatalyst. *J. Am. Chem. Soc.* **142**, 12708–12714 (2020).
14. Hoyle, C. E. & Bowman, C. N. Thiol–ene click chemistry. *Angew. Chem. Int. Ed.* **49**, 1540–1573 (2010).
15. Tondreau, A. M. et al. Iron catalysts for selective anti-Markovnikov alkene hydrosilylation using tertiary silanes. *Science* **335**, 567–570 (2012).
16. Li, H., Shen, S.-J., Zhu, C.-L. & Xu, H. Direct intermolecular anti-Markovnikov hydroazidation of unactivated olefins. *J. Am. Chem. Soc.* **141**, 9415–9421 (2019).
17. Saper, N. I. et al. Nickel-catalysed anti-Markovnikov hydroarylation of unactivated alkenes with unactivated arenes facilitated by non-covalent interactions. *Nat. Chem.* **12**, 276–283 (2020).
18. Wilger, D. J., Grandjean, J.-M. M., Lammert, T. R. & Nicewicz, D. A. The direct anti-Markovnikov addition of mineral acids to styrenes. *Nat. Chem.* **6**, 720–726 (2014).
19. Hu, X., Zhang, G., Bu, F. & Lei, A. Visible-light-mediated anti-Markovnikov hydration of olefins. *ACS Catal.* **7**, 1432–1437 (2017).
20. Margrey, K. A. & Nicewicz, D. A. A general approach to catalytic alkene anti-Markovnikov hydrofunctionalization reactions via acridinium photoredox catalysis. *Acc. Chem. Res.* **49**, 1997–2006 (2016).
21. Kharasch, M. S. & Mayo, F. R. The peroxide effect in the addition of reagents to unsaturated compounds. I. The addition of hydrogen bromide to allyl bromide. *J. Am. Chem. Soc.* **55**, 2468–2496 (1933).
22. Blanksby, S. J. & Ellison, G. B. Bond dissociation energies of organic molecules. *Acc. Chem. Res.* **36**, 255–263 (2003).
23. Mayo, F. R. Free radical addition and transfer reactions of hydrogen chloride with unsaturated compounds. *J. Am. Chem. Soc.* **76**, 5392–5396 (1954).
24. Stanbury, D. M. in *Advances in Inorganic Chemistry* Vol. 33 (ed. Sykes, A. G.) 69–138 (Academic, 1989).
25. Romero, N. A. & Nicewicz, D. A. Organic photoredox catalysis. *Chem. Rev.* **116**, 10075–10166 (2016).
26. Shono, T., Chuankamnerdkarn, M., Maekawa, H., Ishifune, M. & Kashimura, S. Electroorganic chemistry; 145: coupling reaction of an olefin with a radical $NO_3^{\cdot}$ generated by anodic oxidation of NO_3^-. *Synthesis* **85**, 895–897 (1994).
27. Nguyen, V. T. et al. Alkene synthesis by photocatalytic chemoenzymatically compatible dehydrodecarboxylation of carboxylic acids and biomass. *ACS Catal.* **9**, 9485–9498 (2019).
28. Nguyen, V. T. et al. Visible-light-enabled direct decarboxylative N-alkylation. *Angew. Chem. Int. Ed.* **59**, 7921–7927 (2020).

29. Ohkubo, K., Fujumoto, A. & Fukuzumi, S. Metal-free oxygenation of cyclohexane with oxygen catalyzed by 9-mesityl-10-methylacridinium and hydrogen chloride under visible light irradiation. *Chem. Commun.* **47**, 8515–8517 (2011).
30. Romero, N. A. & Nicewicz, D. Mechanistic insight into the photoredox catalysis of anti-Markovnikov alkene hydrofunctionalization reactions. *J. Am. Chem. Soc.* **136**, 17024–17035 (2014).
31. McManus, J. B., Griffin, J. D., White, A. R. & Nicewicz, D. Homobenzylic oxygenation enabled by dual organic photoredox and cobalt catalysis. *J. Am. Chem. Soc.* **142**, 10325–10330 (2020).
32. Finn, M., Friedline, R., Suleman, N. K., Wohl, C. J. & Tanko, J. M. Chemistry of the *t*-butoxyl radical: evidence that most hydrogen abstractions from carbon are entropy-controlled. *J. Am. Chem. Soc.* **126**, 7578–7584 (2004).
33. Giedyk, M. et al. Photocatalytic activation of alkyl chlorides by assembly-promoted single electron transfer in microheterogeneous solutions. *Nat. Cat.* **3**, 40–47 (2020).
34. Lee, G. S., Kim, D. & Hong, S. H. Pd-catalyzed formal Mizoroki–Heck coupling of unactivated alkyl chlorides. *Nat. Commun.* **12**, 991 (2021).
35. Chen, K. S., Tang, D. Y. H., Montgomery, L. K. & Kochi, J. K. Rearrangements and conformations of chloroalkyl radicals by electron spin resonance. *J. Am. Chem. Soc.* **96**, 2201–2208 (1974).

Acknowledgements

We thank N. Haupt, D. Kampen, S. Marcus, F. Kohler and D. Margold (MPI für Kohlenforschung) for the high-resolution mass spectrometry analysis. We thank S. Kestermann (MPI für Kohlenforschung) for the HPLC purification. We thank M. Meyer (MPI für Kohlenforschung) for help in the Stern–Volmer quenching experiments. We thank L. Zhang, Y. Cai, K. Bohdan, A. Hamad, E. de Pedro Beato and B. Lansbergen (MPI für Kohlenforschung) for helpful discussion. We acknowledge financial support from the MPI für Kohlenforschung.

Author contributions

X.S. developed the conceptual approach to the project. J.K. and X.S. developed the chemistry and optimized the reaction conditions. J.K. explored the substrate scope for hydrochlorination and hydronitrooxylation. J.K. and B.A.W. conducted the mechanistic experiments. J.K. performed the DFT calculations. J.K., X.S. and T.R. wrote the manuscript. T.R. directed the project.

Funding

Open access funding provided by Max Planck Society.

Competing interests

The authors declare no competing interests.

Additional information

Supplementary information The online version contains supplementary material available at https://doi.org/10.1038/s41929-023-00914-7.

Correspondence and requests for materials should be addressed to Tobias Ritter.

Peer review information *Nature Catalysis* thanks the anonymous reviewers for their contribution to the peer review of this work.